^{23}Na NMR Study of NASICON-type Compounds, $Na_{1+x}Sc_xTi_{2-x}(PO_4)_3$

Hirotsugu Masui, Takahiro Ueda, Keisuke Miyakubo, Taro Eguchi, and Nobuo Nakamura

Department of Chemistry, Graduate School of Science, Osaka University,
Toyonaka, Osaka, 560–0043, Japan

Reprint requests to Prof. N. N.; Fax: +81-6-6850-5785, E-mail: nobuo@ch.wani.osaka-u.ac.jp

Z. Naturforsch. **55 a,** 348–352 (2000); received August 30, 1999

Presented at the XVth International Symposium on Nuclear Quadrupole Interactions, Leipzig, Germany, July 25 - 30, 1999.

The structure of NASICON-type compounds, $Na_{1+x}Sc_xTi_{2-x}(PO_4)_3$ ($0 \leq x \leq 2$), and the dynamics of Na^+ have been investigated by ^{23}Na NMR spectroscopy. It was found that the ^{23}Na 1D and 2D MQMAS spectra depend on the Na concentration, suggesting strongly that the Na^+ ions are distributed between two crystallographically nonequivalent sites, one is a special position with axial symmetry, and the other a position of low symmetry. The chemical exchange between these different sites in the crystal takes place at room temperature, which may cause the high Na ion conduction of this material.

Key words: NASICON; Superionic Conductor; 2D MQMAS NMR; Chemical Exchange.

1. Introduction

"NASICON" is an acronym of "**Na** Super **I**onic **CON**ductor" and denotes mainly $Na_{1+x}Zr_2(SiO_4)_x(PO_4)_{3-x}$, which were first synthesized by Hong *et al.* with a very clever idea of crystal engineering[1, 2], but presently the name is generally used for materials which have similar structures as the original NASICON. The general formula of NASICON-type materials is hence $Na_{1+x}M^{III}_xM^{IV}_{2-x}(PO_4)_3$.

In NASICON-type crystals, the PO_4 tetrahedra share their oxygens with MO_6 (M = M^{III} or M^{IV}) octahedra, building a three-dimensional network with space group $R\bar{3}c$ (usually the low-conductive phase) or Cc (the high-conductive phase).

When $x = 0$, the crystallographic symmetry is $R\bar{3}c$ and the Na^+ ions occupy 6*b* positions (hereafter named Na(1) sites) on the crystallographic three-fold axis in the unit cell (Figure 1). When $x > 0$, extra (x) Na^+ ions occupy some of the 18*e* positions (Na(2) sites). Since these non-equivalent sites are arranged alternatively, and even when x reaches the highest value (= 2) by substitution of all tetra-valent cations (M^{IV}) by the tri-valent cations (M^{III}), there are still the inherent vacancies at Na(2) sites. These vacant sites can be used for the exchange of Na^+ between neighbouring Na(1) and Na(2) sites and thus for the long-range transport of Na^+ cations.

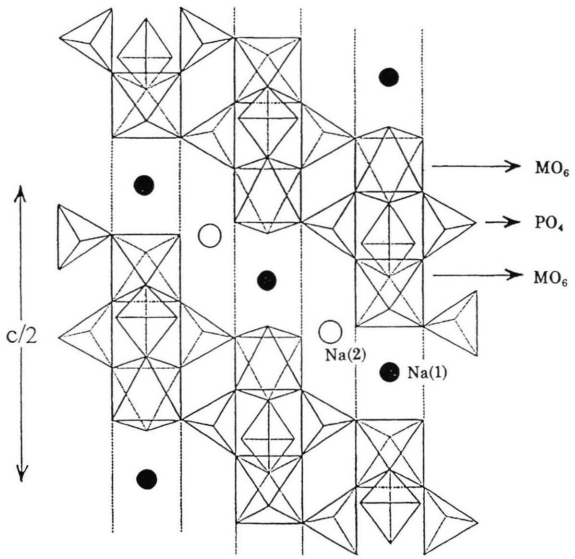

Fig. 1. Structure of NASICON-type compounds [24].

A number of structural studies using ^{23}Na, ^{31}P, and ^{29}Si NMR spectra have been conducted on the present material [3 - 10]. Since ^{23}Na is a quadrupolar nucleus, its NMR spectra in NASICON may provide

0932–0784 / 00 / 0100–0348 $ 06.00

very useful information on the static and dynamic nature of the material.

However, it is usually more difficult to derive valuable information from NMR experiments on NASICON-type materials than on LISICON, lithium superionic conductor. One reason for this difficulty is that the quadrupole interaction is usually large for ^{23}Na and results in a very broad spectrum. It is sometimes quite difficult to elucidate certain quadrupole interaction parameters from such a broad spectrum, especially when the sample contains two or more nonequivalent Na ions. New NMR methods to overcome this difficulty were developed, such as Magic-Angle Spinning(MAS) NMR and 2D Nutation NMR, and have been successfully applied [11]. However, it was also found that even 2D Nutation NMR spectra were yet too complicated to be analyzed reasonably for some materials [12].

The present work deals with the local structure of $Na_{1+x}Sc_xTi_{2-x}(PO_4)_3$ ($0 \leq x \leq 2$) and the dynamics of Na^+ cations in the material, using ^{23}Na solid-state NMR spectroscopy including a new high-resolution NMR method for quadrupolar nuclei, *i. e.*, Multiple Quantum Magic-Angle Spinning (MQMAS) experiments.

2. Experimetal

Samples of $Na_{1+x}Sc_xTi_{2-x}(PO_4)_3$ with various values of x were synthesized by calcination of the stoichiometric mixture of Na_2CO_3, TiO_2(anatase), Sc_2O_3, and $NH_4H_2PO_4$. All the samples were thoroughly ground and sintered at 1000 - 1100 °C for 5 hours. The sintering process for each sample was repeated three or four times until extra reflections in the powder X-ray diffraction (XRD) pattern were diminished.

Differential thermal analysis was carried out on each sample between 77 and 400 K. No phase transition was detected except for $Na_3Sc_2(PO_4)_3$ ($x = 2$), which undergoes a phase transition at 335 K, as has been reported [13 - 19].

The impedance of all samples was measured by a Hewlett-Packerd 4192A LF impedance analyzer. For the measurements the samples were formed into cylindrical pellets ($\approx$ 10 mm ø$\times$ 2 - 3 mm) by pressing and heated at 1150°C for 1 hour. Au electrodes were formed on both faces of the pellets by vacuum evaporation. The temperature was controlled to within $\pm$3K in the range from room temperature up to 700 K.

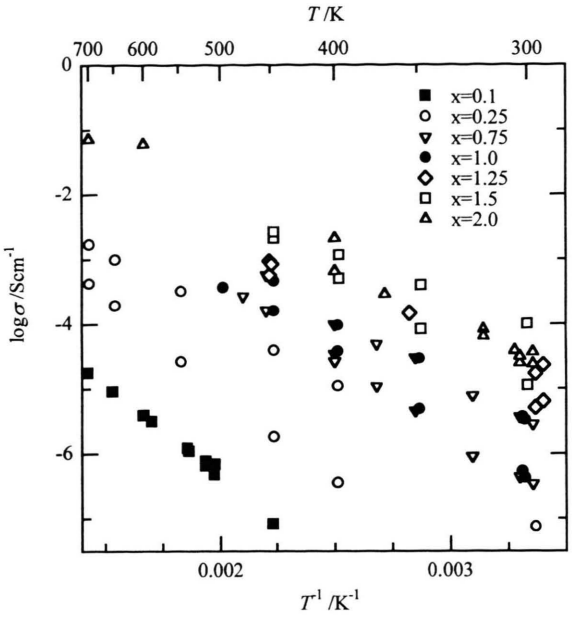

Fig. 2. Conductivity of $Na_{1+x}Sc_xTi_{2-x}(PO_4)_3$.

The conductivity of each sample was deduced from the impedance data by the use of the program "Equivalent Circuit" written by Boukamp [20], where it is assumed that an equivalent circuit of the measured system can be constructed by a series of one or two simple circuits in which a resistance is arranged in parallel to be a constant phase element (CPE) [21].

The ^{23}Na NMR spectra were measured by a Bruker DSX-200 spectrometer with a resonance frequency of 52.937 MHz. Powdered NaCl was used for the chemical shift reference. The 1D static spectra were measured by a spin-echo sequence with suitable soft pulses ($\nu_1 \sim$ 16kHz) [22]. The sample spinning rate for the MAS and MQMAS spectra was between 4 and 12.5 kHz. Also ^{31}P MAS spectra were measured for the characterization of the samples.

3. Results and Discussion

The XRD powder patterns indicate that the space groups of the samples are $R\bar{3}c$ for $0 \leq x \leq 1.75$ and Cc for $x = 2$, being similar to the crystal structure of Hong's NASICON. When $x = 0$, the lattice parameters of the $R\bar{3}c$ cell are a = 0.8457(5) nm and c = 2.1780(3) nm. Both a and c lengthen with increase in x and reach a = 0.879(1) nm and c = 2.30(1) nm at $x = 1.75$.

Table 1. Arrhenius parameters for the ionic conductivities of $Na_{1+x}Sc_xTi_{2-x}(PO_4)_3$.

x	σ_0/Scm^{-1}	E_a/kJmol^{-1}
0.1	0.20 ± 0.01	53 ± 3
0.25	3.3 ± 0.3	43 ± 4
	4.7 ± 0.2	55 ± 2
0.75	8.8 ± 0.5	37 ± 2
	23 ± 2	45 ± 3
1.0	7.7 ± 0.5	37 ± 2
	17 ± 1	43 ± 2
1.25	1.4 ± 0.2	27 ± 2
	7.5 ± 1.4	34 ± 6
1.5	1.3 ± 0.1	23 ± 1
	150 ± 9	41 ± 2
2.0	66 ± 23	36 ± 12
	30 ± 12	35 ± 14

Two values of σ_0 and E_a for each sample (except $x = 0.1$) correspond to the bulk (higher conductivity) and the grain boundary (lower conductivity), respectively.

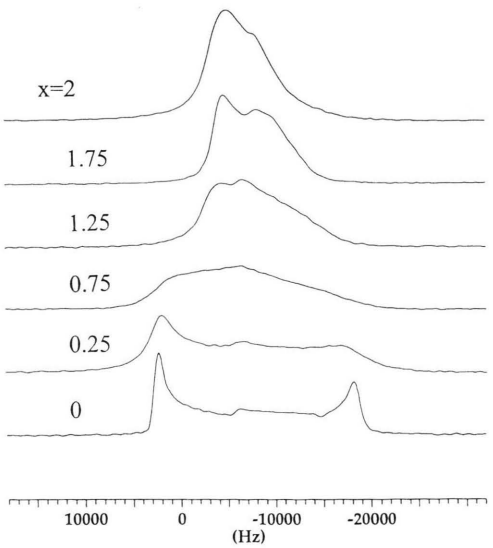

Fig. 3. ^{23}Na static spectra of $Na_{1+x}Sc_xTi_{2-x}(PO_4)_3$.

The temperature dependence of the conductivity at each composition is shown in Figure 2. The conductivity of the compounds increases with increase in x. The conductivity obeys the Arrhenius activation process, $\sigma = \sigma_0 \exp(-E_a/RT)$. The parameters σ_0 and E_a are summerized in Table 1.

Figure 3 shows the ^{23}Na 1D spectra taken by the spin-echo method at room temperature. The spectrum for $x = 0$ consists of a typical second order quadrupolar pattern with a quadrupole coupling constant (QCC) of 1.5 ± 0.1 MHz and with an asymmetry parameter (η) of the electric field gradient of 0 ± 0.05. This result is consistent with the XRD results that only the special (axial) position(Na(1)) is populated and all the low symmetry sites(Na(2)) are empty. Each ^{23}Na 1D spectrum for finite x consists of the superposition of two components originated from the two non-equivalent sites, and as a result the line shape varies with the Na content. However, it is difficult to evaluate the values of QCC and η for both Na(1) and Na(2) because there are many parameters to be fixed simultaneously, *i. e.*, the quadrupole interaction parameters, the chemical shifts and their anisotropies, the relative intensities of the individual components, and the broadening factors.

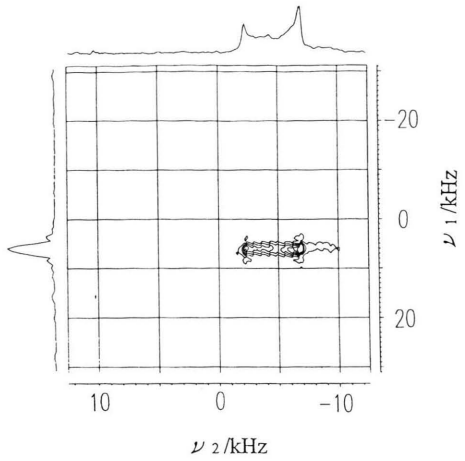

Fig. 4. MQMAS spectrum of $NaTi_2(PO_4)_3$.

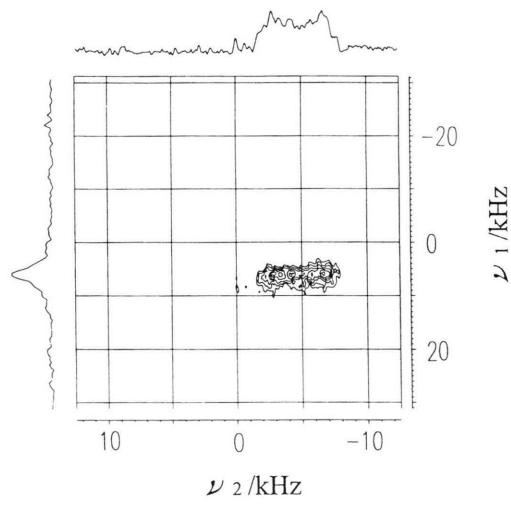

Fig. 5. MQMAS spectrum of $Na_{1.25}Sc_{0.25}Ti_{1.75}(PO_4)_3$ at room temperature.

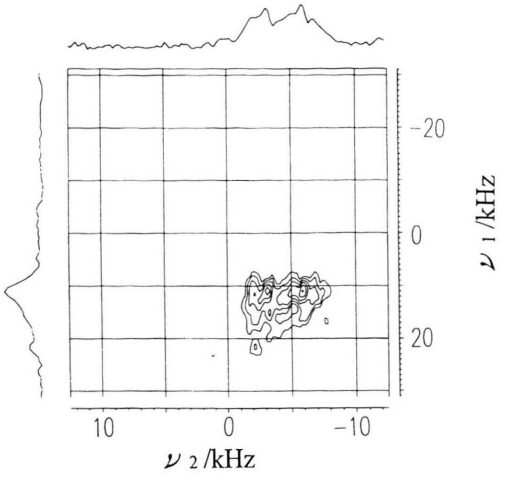

Fig. 6. MQMAS spectrum of $Na_{1.25}Sc_{0.25}Ti_{1.75}(PO_4)_3$ at 180 K.

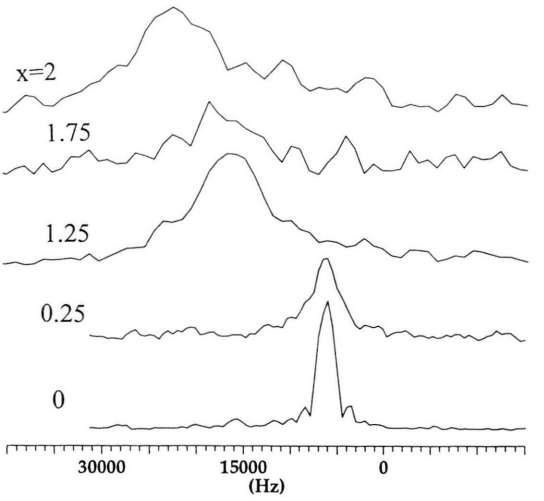

Fig. 7. F_1 Projection of MQMAS spectra.

In order to simplify the above complex spectrum and to obtain reliable values of the QCC and η at both Na sites, we applied ^{23}Na 2D MQMAS NMR measurements to the present materials. Figure 4 is the MQMAS spectrum of the sample with $x = 0$. A slight distortion of the lineshape in the F_2 projection was observed. This spectrum supports the assumption that only one Na site is populated. The frequency shift on the F_1 axis is contributed by both the isotropic chemical shift and the quadrupolar term in the simplest case where a single crystallographic position exists. According to the theoretical treatment of the MQMAS the net shift along the F_1 axis is represented by [23]

$$\nu^{F1} = \frac{1}{8} \times \frac{\nu_Q^2}{\nu_0}\left(\frac{\eta^2}{3} + 1\right) + \frac{17}{8}\delta\nu_{CS}^{iso}, \qquad (1)$$

where $\nu_Q = e^2Qq/2h$, ν_0 is the ^{23}Na Larmor frequency and $\delta\nu_{CS}^{iso}$ the isotropic chemical shift. By analyzing the spectrum with this equation, the isotropic chemical shift for Na(1) is determined to be $+6.0 \pm 0.1$ ppm.

For the sample with finite x, the MQMAS spectrum at room temperature (Fig. 5) depends on x but cannot be considered to be any simple superposition of the two or more components, reflecting probably a fast exchange process between two sites. To ascertain the existence of such an exchange, we carried out MQMAS experiments on some samples at low temperature(180K) (Figure 6). The peak on the F_1 projection consists of two signals separated by about 3.5 kHz, implying that the exchange rate becomes slow at low temperatures.

Figure 7 shows the dependence of the F_1 projection of the MQMAS spectrum on x. The peak shifts with x and, if we assume that this shift is brought by the fast mixing of two peaks which are originally located at different frequencies, a QCC value for the Na(2) site is estimated to be 2 - 3 MHz by referring to the above value of QCC = 1.5 MHz and $\eta = 0$ for the Na(1) site. The fact that η is nearly 1 was deduced from the 1D spectra (Figure 3). These estimations are reasonably understood by consideration of the crystallographic symmetry of the sites.

[1] H. Y.-P. Hong, Mater. Res. Bull. **11**, 173 (1976).
[2] J. B. Goodenough, H. Y-P. Hong, and J. A. Kafalas, Mater. Res. Bull. **11**, 203 (1976).
[3] C. Jäger, S. Barth, and A. Feltz, Chem. Phys. Lett. **154**, 45 (1989).
[4] E. R. Losilla, M. A. G. Aranda, S. Bruque, M. A. París, J. Sanz, and A. R. West, Chem. Mater. **10**, 665 (1998).
[5] C. Jäger, G. Scheler, U. Sternberg, S. Barth, and A. Feltz, Chem. Phys. Lett. **147**, 49 (1988).
[6] C. Jäger, S. Barth, and A. Feltz, Chem. Phys. Lett. **150**, 503 (1988).
[7] C. Jäger, G. Scheler, S. Barth, and J. A. Feltz, Exper. Technik der Physik **36**, 339 (1988).
[8] N. Gasmi, N. Gharbi, H. Zarrouk, P. Barboux, R. Morineau, and J. Livage, J. Sol-Gel Sci. Tech. **4**, 231 (1995).
[9] Y. Yue, F. Deng, H. Hu, C. Ye, Z. Lin, and S. Tian, Mater. Chem. Phys. **37**, 86 (1994).

[10] K. C. Sobha and K. J. Rao, J. Solid State Chem. **121**, 197 (1996).
[11] H. Ohki and N. Nakamura, Z. Naturforsch. **47a**, 319 (1992).
[12] N. Nakamura, Z. Naturforsch. **49a**, 337 (1994).
[13] C. J. Delbecq, S. A. Marshall, and S. Susman, Solid State Ionics **1**, 145 (1980).
[14] J. P. Boilot, G. Collin, and R. Comes, Solid State Ionics **5**, 307 (1981).
[15] S. Susman, C. J. Delbecq, and T. O. Brun, Solid State Ionics **9&10**, 839 (1983).
[16] D. Tran Qui, J. J. Capponi, M. Gondrand, and J. C. Joubert, Solid State Ionics **5**, 305 (1981).
[17] G. Collin, R. Comes, J. P. Boilot, and Ph. Colomban, J. Phys. Chem. Solids **47**, 843 (1986).
[18] M. Barj, H. Perthuis, and Ph. Colomban, Solid State Ionics **9&10**, 845 (1983).
[19] V. V. Tkachev, V. I. Ponomarev, and L. O. Atovmyan, Zh. Strukt. Khim. **25**, 11(1984).
[20] B. A. Boukamp, Solid State Ionics **11**, 39 (1984).
[21] Impedance Spectroscopy, Emphasizing Solid Materials and Systems, ed. J. Ross MacDonald, John Wiley & Sons, New York 1987.
[22] Y. Dumazy, J.-P. Amoureux, and C. Fernandez, Mol. Phys. **90**, 959 (1997).
[23] D. Massiot, B. Touzo, D. Trumeau, J. P. Coutures, J. Virlet, P. Florian, and P. J. Grandinetti, Solid State Nucl. Magn. Reson. **6**, 73 (1996).
[24] R. Futagami, Hydrothermal Synthesis of Alkaline Transition Metal Phosphates. PhD thesis, Osaka University 1994.